THE PLASMA ENVIRONMENT AROUND MERCURY

Réjean Grard and Harri Laakso
Space Science Department of ESA, ESTEC, Noordwijk, The Netherlands
Phone: +31 71 565 3596 and -3319, fax: +31 71 565 4697,
email: Rejean.Grard@esa.int and Harri.Laakso@esa.int

Abstract

Our understanding of the plasma environment of planet Mercury is mostly derived from the limited amount of data which has been collected by the NASA flyby mission, Mariner 10, in 1974-1975. The prospect for new missions, the NASA Messenger orbiter and the ESA BepiColombo cornerstone have, however, stimulated a renewed interest in this planet. Like the Moon, Mercury has a vestigial atmosphere and no ionosphere, but - against all expectations - it possesses a small, but definite, intrinsic magnetic field. Due to the weakness of this field, of the order of a few 100 nT at the equator, and the relatively high solar wind pressure which prevails at the orbit of Mercury, the size of the magnetospheric cavity is much smaller than that of the Earth. The two environments have somewhat similar topologies but their dynamics differ widely. The solar wind may even reach the surface of Mercury when its pressure is sufficiently large. The formation of radiation belts is probably impeded for lack of a sufficiently strong magnetic confinement. The environment is permeated by a current system which is basically unknown and the plasma is rarefied, like in the Earth magnetosphere. Due to the proximity of the Sun, the emission rate of photoelectrons is up to 10 times larger than at the Earth orbit and leads to unique electrostatic phenomena on orbiting spacecraft and at the surface of the planet.

1. Introduction

Mercury is a small but important object because it forms with Venus, Earth and Mars the family of the terrestrial planets (Figure 1). Each member of this group carries information that is essential for retracing the history of the whole set and constraining the theories of planetary formation and evolution.

Even before the space era, the mass of Mercury was known to be abnormally high for its size, due to the perturbation that it induces on the motion of nearby asteroids. The density of Mercury is indeed out of line with those of the other terrestrial planets, including the Moon (Figure 2), an oddity which is not easily explained by current theories.

Mercury is the closest planet to the Sun and is hard to see from the ground or even from the Earth orbit. Nor is inserting a spacecraft around Mercury an easy task, due to the gravitational potential and the thermal burden of the Sun.

No spacecraft has ever orbited Mercury but the American probe Mariner 10 made three flybys of this planet in 1974-1975 and obtained images of somewhat less than half the surface (Figure 3).

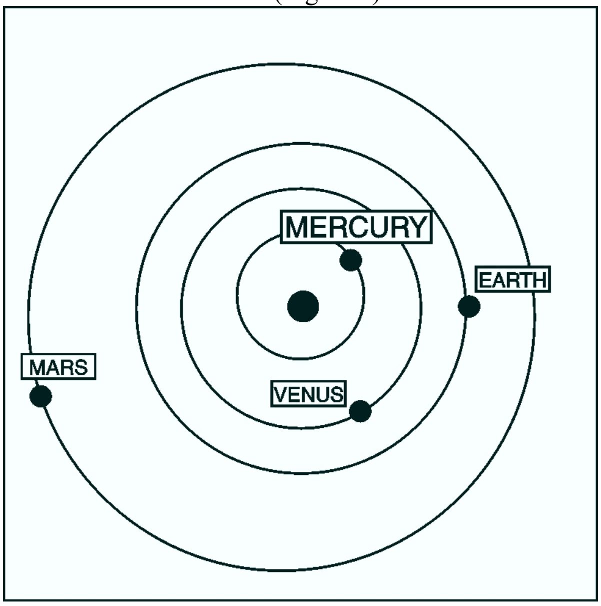

Figure 1: The terrestrial planets.

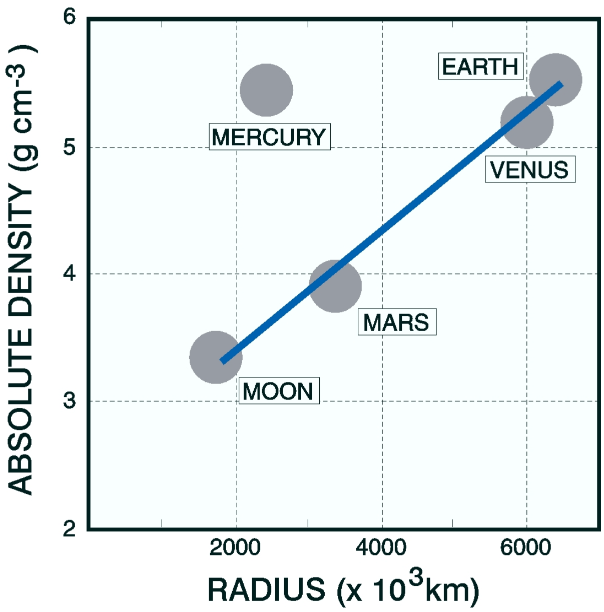

Figure 2: Density of the terrestrial planets and the Moon.

Figure 3: Hemisphere of Mercury imaged by Mariner 10 (no data from the blank areas).

2. The Magnetospheric Environment

Mariner 10 discovered that, against all expectation, the planet had a magnetic field (Ness et al., 1977). This was contradicting the earlier assumption that the core was frozen and that Mercury, like the Moon, could not support any internal dynamo.

Figure 4 represents the path of Mariner 10 during the first and third flybys, on 29 March 1974 and 16 March 1975. The plots on the left-hand side are the cylindrical projections of the in-bound and out-bound legs; the revolution axis is aligned along the sunward direction. The right-hand side panel shows the projections of the trajectories in the plane normal to this axis. The spacecraft altitudes are 707 km and 327 km on the first and third closest approaches (CA), respectively (Russell et al., 1988).

The locations of the observed bow shock (BS) and magnetopause (MP) crossings are indicated, superimposed on a scaled model of these boundaries. The magnetopause is the envelope of the planetary magnetic field and the bow shock results from the interaction between the supersonic solar wind and the obstacle formed by the magnetized planet. None of these boundaries were crossed during the second flyby, on 21 September 1974, because the closest approach took place at a planetocentric distance larger than 20 Mercury radii in the sunward direction.

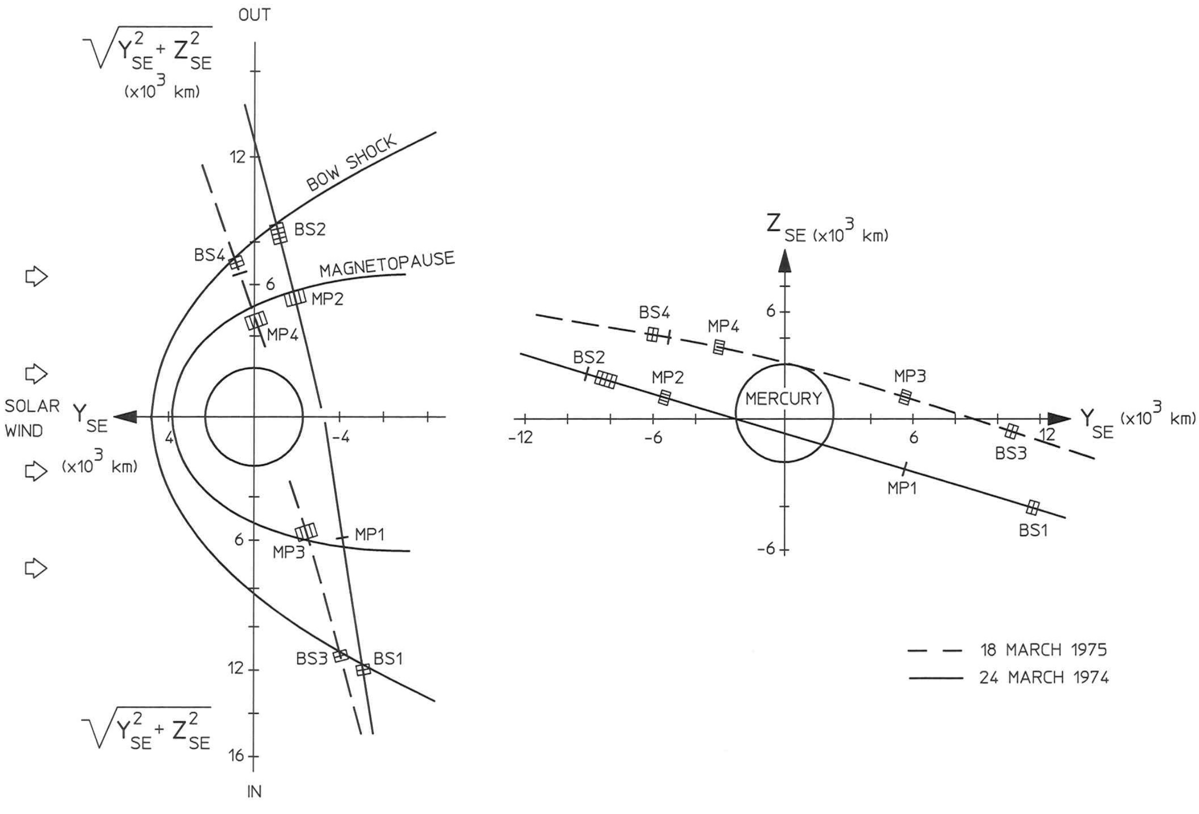

Figure 4: Trajectories of Mariner 10 during the first and third flybys (after Russell et al., 1988).

The modulus of the magnetic field recorded during the last flyby is plotted in Figure 5. A model of the magnetosphere for a dipolar field structure is depicted in Figure 6 (Slavin et al., 1997), by analogy with the Earth environment. The strength of the field is of the order of 300 nT at the equator, 100 times less than at Earth, and the size of the magnetosphere is about 5% of that of Earth. It has been estimated that, during 6% of the time, the solar wind exerts a pressure larger than the planetary field and strikes the surface (Russell et al., 1988).

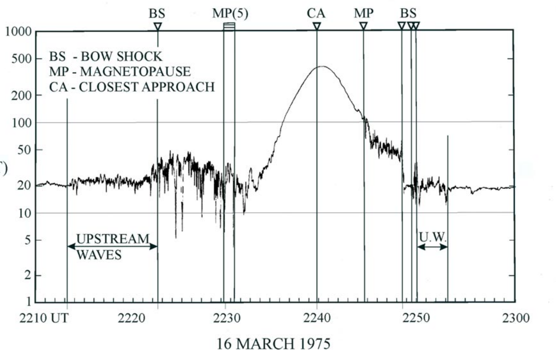

Figure 5: Modulus of the magnetic field observed during the third Mariner 10 flyby (after Ness et al., 1976).

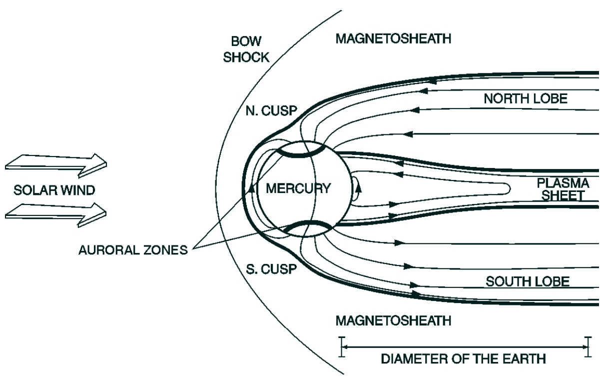

Figure 6: The magnetosphere of Mercury (after Slavin et al., 1977, and Grande et al., 2001).

The electron density observed during the first flyby, is shown in Figure 7 (Ogilvie et al., 1977); it is about 10-20 cm^{-3} in the solar wind and in the magnetosheath, as expected when Mercury is at aphelion. The magnetospheric plasma is rarefied and the electron density, of the order of 5 cm^{-3} on an average, can be lower than 1 cm^{-3}, like in the Earth magnetosphere. The electron typical energies lie in the range 100-1000 eV, one to two orders of magnitude larger than in the solar wind.

Mercury, like the Moon, has a vestigial atmosphere due to ion and photon sputtering and micrometeorite vaporisation. This gaseous environment is best described as an exosphere. The mean free paths are large; the density and composition are highly variable (Killen and Ip, 1999).

3. Particle Trapping and Precipitation

The efficiency of a magnetized environment for trapping charged particles can be quantified locally by the angle of the loss cone which contains the pitch directions of the particles precipitating on the planet's surface.

The loss cone at the magnetic equator is shown in Figure 8 for a dipolar field, with the approximate locations of the subsolar Earth and Mercury magnetopauses. It is seen that, in a first approximation, the cone angles at Mercury are always expected to lie above the range which characterizes the radiation belts at Earth.

This surmise is corroborated by a more realistic model which includes the magnetopause and tail currents, in addition to the dipolar field. Figure 9 shows the isocontours of the loss cone angles in the magnetic equatorial plane and confirms that this angle is always larger than about 35° on closed magnetic shells in the sunward hemisphere. The existence of permanently trapped particle population is therefore unlikely (Grard et al., 1999).

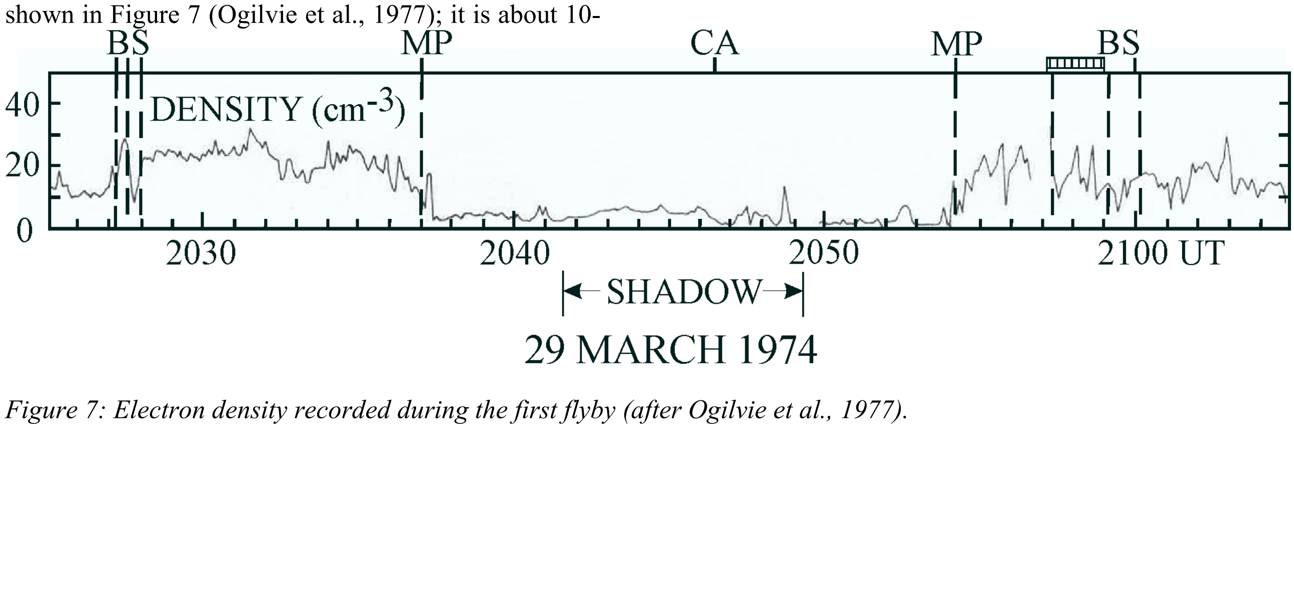

Figure 7: Electron density recorded during the first flyby (after Ogilvie et al., 1977).

4. Electric Phenomena and Surface Interactions

4.1 Orbiting Spacecraft

Magnetospheric plasma densities of 1-5 cm^{-3} and thermal energies of 100-1000 eV yield ambient electron random current densities of 0.27 to 4.2 :A m^{-2}. On the other hand, the saturation photoelectron current density emitted from a surface element exposed to sunlight under normal incidence, j_{ph}, depends on the nature of the material and the distance from the Sun; it can reach 90-200 :A m^{-2}, at least (Grard, 1997).

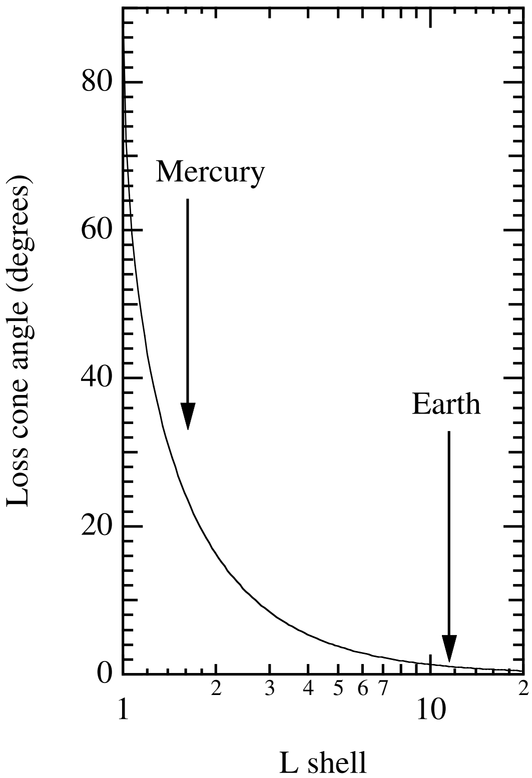

Figure 8: Loss cone angle at the magnetic equator vs. L shell parameter for a dipolar field.

The floating electric potential of an illuminated surface element N_f N_O ln (j_{ph}/j_e), where N_O= 1.6 eV is the mean kinetic energy of the photoelectrons, is therefore positive and of the order of 5-10 V (see also Torkar et al., 1997).

The equilibrium potential is much dependent upon the distribution of the most energetic photoelectrons and larger levels can be expected, as evidenced by one of the electron spectrum collected during the third flyby and shown in Figure 10. The floating potential is +40 V and two electron populations can be clearly differentiated. On the one hand, the photoelectrons emitted from the spacecraft with energies less than 40 eV are returned to the analyser. On the other hand, the ambient electrons are accelerated by the positive potential of the spacecraft and their apparent energies are larger than 40 eV (Ogilvie et al., 1977). Taking into account this 40 eV energy shift, the ambient electron density is estimated to be 7 cm^{-3}. Spacecraft charging of up to 90 V have been reported.

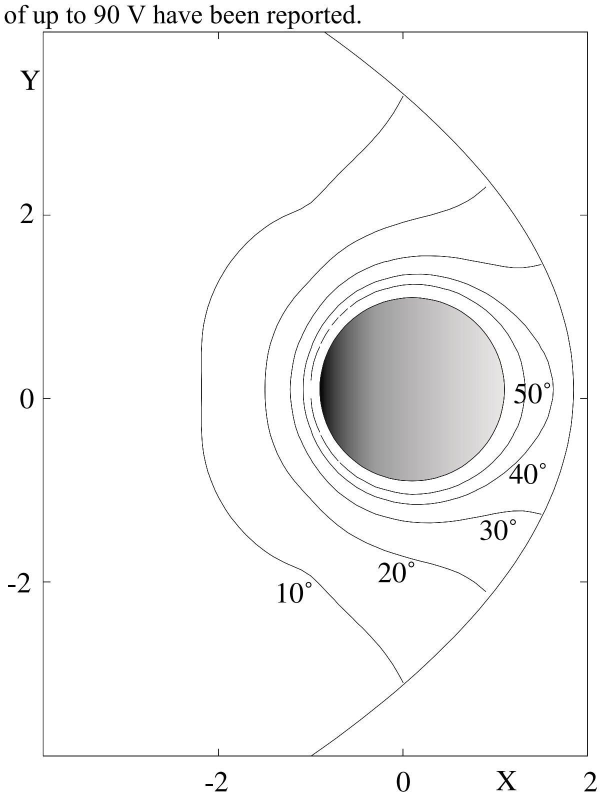

Figure 9: Isocontours of the loss cone angles in the equatorial plane (distances in Mercury radii).

Insulated surface elements in shadow will, of course, develop negative potentials of possibly several 100 V, commensurate with the thermal energy of the ambient electrons. Differential charging might therefore be expected on spacecraft with insufficient surface conductivity.

4.2 Planetary Surface

Photoemission also induces electric phenomena on the surface of Mercury which are specific to bodies without any atmosphere. The saturation photoelectron current emitted by the sunlit area lies in the range 2-4 GA. To set the ideas, this flow is 6.5 times larger in magnitude than that of the solar ions or electrons which impact the cross-section area of the magnetopause.

Photoelectrons play a role in current exchanges between the planet and its environment and insure the coupling between subsurface and magnetospheric currents (Figure 11). The photoelectron layer is also characterised by a horizontal conductance of the order of 10^{-5} S, larger than that of the height-integrated transverse conductivity of the exosphere (Grard, 1997).

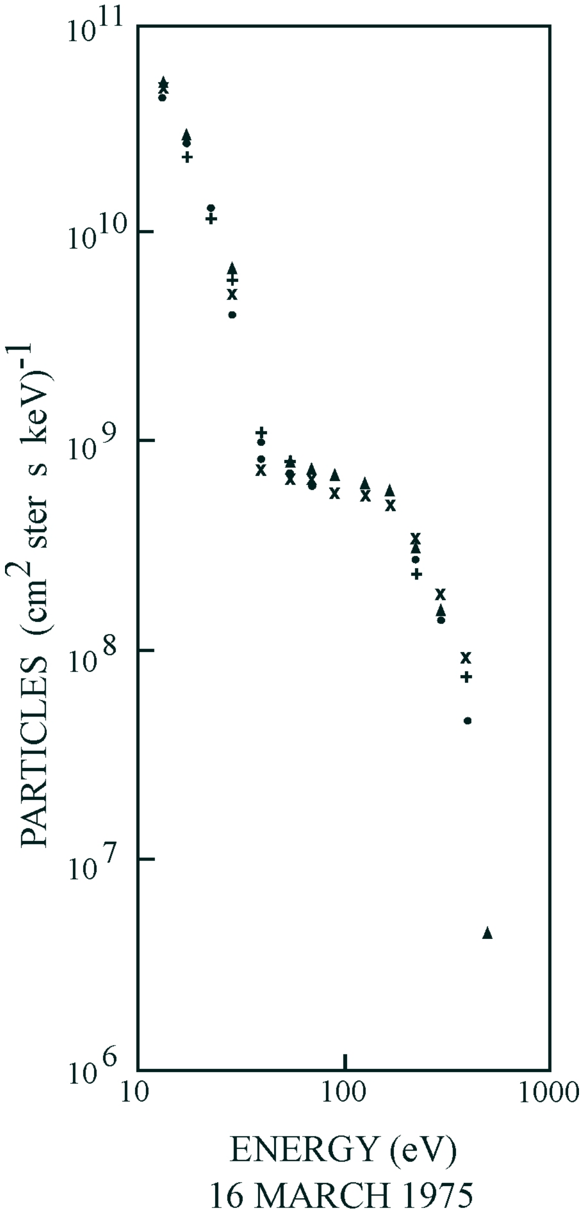

Figure 10: Effect of spacecraft charging on an electron spectrum recorded during the third Mariner 10 flyby.

The precipitation of energetic particles on the surface in the high latitude regions, analogous to the auroral zones on Earth, is a potential source of X-ray radiation (Grande et al., 2001).

5. CONCLUSION

A better understanding of Mercury's environment is all the more important as several spacecraft will orbit this planet and land on its surface toward the end of this decade.

The NASA Messenger spacecraft is presently under development; it will be launched in 2004 and arrive at Mercury in April 2009. The ESA mission BepiColombo will be launched in August 2009 and arrive at Mercury 3.5 years later, in the current baseline. It consists of a planetary orbiter for remote sensing , a magnetospheric orbiter to be procured by Japan and a lander.

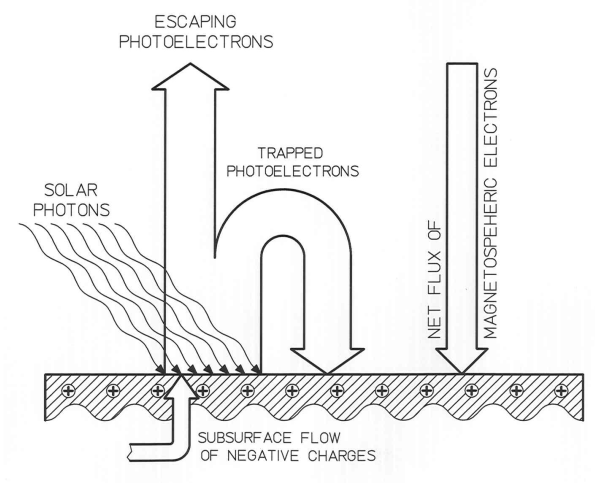

Figure 11: Charge exchange between the surface of Mercury and the magnetospheric environment.

References

Grande M., Dunkin S.K. and Kellett B., Opportunities for X-ray science at Mercury, *Planet. Space Sci.*, in press, 2001.

Grard, R., Photoemission on the surface of Mercury and related electrical phenomena, *Planet. Space Sci.*, **45**, 67-72, 1997.

Grard R., Laakso H. and Pulkkinen T.I., The role of photoemission in the coupling of the Mercury surface and ionosphere, *Planet. Space Sci.*, **47**, 1459-1463, 1999.

Killen R.M. and Ip W.-H., The surface-bounded atmospheres of Mercury and the Moon, *Rev. Geophys.*, **37(3)**, 361-406, 1999.

Ness N.F., Behannon K.W., Lepping R.P. and Whang Y.C., Observations of Mercury's magnetic field, *Icarus*, **28**, 479-488, 1976.

Ogilvie K.W., Scudder J.D., Vasyliunas V.M., Hartle R.E. and Siscoe G.L., Observation at the Planet Mercury by the Plasma Electron Experiment: Mariner 10, *J. Geophys. Res.*, **82(13)**, 1807-1824, 1977.

Russell C.T., Baker D.N. and Slavin J.A., The magnetosphere of Mercury, In *Mercury*, eds. F. Vilas, C.R. Chapman and M.S. Matthews, pp. 514-561. University of Arizona Press, Tucson, 1988.

Slavin J.A., Owen J.C.J. Connerney J.E.P., Christon S.P., Mariner 10 observations of field-aligned currents at Mercury, *Planet. Space Sci.*, **45**, 133-141, 1997.

Torkar K., Fehringer M., Rüdenauer F., Grard R. and Riedler W., Necessity and feasibility of spacecraft potential control in the hermean magnetosphere, *Planet. Space Sci.*, **45**, 149-161, 1997.